BAREKENG: Journal of Mathematics and Its Applications
June 2026 Volume 20 Issue 2 Page 1659–1674
P-ISSN: 1978-7227 E-ISSN: 2615-3017
https://doi.org/10.30598/barekengvol20iss2pp1659-1674

SOIL MOISTURE PREDICTION USING LSTM AND GRU: UNIVARIATE AND MULTIVARIATE DEEP LEARNING APPROACHES

Jemsri Stenli Batlajery [1*], **Agus Buono** [2], **Mushthofa Mushthofa** [3]

[1,2,3]*School of Data Science, Department of Mathematics and Computer Science, IPB University*
Jln. Meranti, IPB Dramaga Campus, Bogor, 16680, Indonesia

*Corresponding author's e-mail: * **jemsribatlajery@apps.ipb.ac.id***

Article Info

Article History:

Received: 16th July 2025
Revised: 29th July 2025
Accepted: 21st August 2025
Available Online: 26th January 2026

Keywords:

Deep learning;
Gated Recurrent Unit;
Long Short-Term Memory;
Soil moisture.

ABSTRACT

Soil moisture is an important indicator in the management of water resources, precision agriculture, and disaster mitigation, such as drought and land fires. Fluctuations in soil moisture are influenced by various climate variables, requiring a reliable predictive approach essential. This research develops a daily soil moisture prediction model using Long Short-Term Memory (LSTM) and Gated Recurrent Unit (GRU) algorithms with univariate and multivariate approaches. Soil moisture data were obtained from Google Earth Engine, while climate data were collected from 10 BMKG stations in East Java for the period 2019–2024. Data preprocessing includes cubic spline interpolation to handle missing values and Min-Max normalization to achieve uniform feature scaling. Models were built using a direct forecasting approach for horizons t *to* $t+9$ *and five evaluation metrics: MAE, MSE, RMSE, MAPE, and* R^2*. The results show that the multivariate GRU model performs best at horizon* $t+9$ *with MAE = 0.05455, MSE = 0.00604, RMSE = 0.07539, MAPE = 0.19280, and* R^2 *= starting from 0.9626 on day 1 (t), then decreasing to 0.8075 on day 10* $(t+9)$*. The univariate LSTM model excelled in training time efficiency (<400 seconds) at most stations. The multivariate GRU model demonstrates the highest accuracy and stability, making it suitable for medium- to long-term forecasting, while the univariate LSTM excels in training speed, making it effective for daily predictions. The model's performance remains limited to the dataset's spatial and temporal scope. Therefore, future research should test the model in other regions and under extreme climate conditions, as well as apply transfer learning in data-scarce areas. The novelty of this study lies in comparing LSTM and GRU performance for daily soil moisture prediction in both univariate and multivariate scenarios, using complete climate variables from multiple stations.*

How to cite this article:

J. S. Batlajery, A. Buono and M. Mushthofa., "SOIL MOISTURE PREDICTION USING LSTM AND GRU: UNIVARIATE AND MULTIVARIATE DEEP LEARNING APPROACHES", *BAREKENG: J. Math. & App.*, vol. 20, no. 2, pp. 1659-1674, Jun, 2026.

Journal homepage: *https://ojs3.unpatti.ac.id/index.php/barekeng/*
Journal e-mail: *barekeng.math@yahoo.com; barekeng.journal@mail.unpatti.ac.id*

Research Article · Open Access

1. INTRODUCTION

Indonesia, as a tropical country, holds significant potential for natural resources but is also vulnerable to climate change due to its diverse geographical conditions [1]. Climate change over the last 150-200 years [2] has had a significant effect on agriculture, water resource management, disaster mitigation, infrastructure development, and ecosystem sustainability [3], [4], [5]. In the agricultural sector, climate change shifts cropping patterns and reduces crop yields. In water management, climate change impacts water quality and availability and increases the risk of natural disasters, requiring better mitigation strategies [6].

One critical component influenced by climate variability is soil moisture, which plays a role in the soil-plant-atmosphere system, hydrology, and climate change [7], [8]. Soil moisture regulates the distribution of precipitation, surface flow, and feedback to the atmosphere [9], so accurate monitoring is essential to support agricultural productivity, disaster mitigation, and ecosystem sustainability [10], [11].

Predicting soil moisture from time-series data is necessary to enable real-time decision-making. Deep learning algorithms such as Long Short-Term Memory (LSTM) and Gated Recurrent Unit (GRU) offer advantages in handling sequential dependencies and addressing the vanishing gradient problem [12], [13], [14]. GRU has a simpler architecture with computational efficiency advantages over LSTM [15], making it a potential alternative for soil moisture prediction.

Research on soil moisture prediction has been extensively conducted using various approaches. [16] employed the Convolutional Neural Network (CNN) algorithm to predict soil moisture based on different soil textures and achieved an R^2 value of 0.983. Although accurate, the study used only a univariate approach and did not consider climatic variables. [17] compared the ARIMA, Random Forest (RF), and LSTM algorithms for regional soil moisture prediction over a three-day horizon. The results indicated that LSTM outperformed the others with a MAPE of 6.76 and MAE of 0.007; however, the study did not comprehensively integrate climatic factors. Meanwhile, [18] implemented an LSTM for multivariate prediction, incorporating climate variables such as rainfall, season, temperature, evapotranspiration, and soil texture. The model achieved a performance of $R^2 = 0.87$ and RMSE $= 0.046$, suggesting that climate is a significant factor in soil moisture prediction.

Although previous studies have successfully developed soil moisture prediction models using various machine learning and deep learning algorithms, several notable limitations remain. Many earlier studies focused solely on univariate prediction and overlooked the influence of key climatic variables, such as rainfall, temperature, humidity, sunlight duration, and wind speed, which play a crucial role in the dynamics of soil moisture. In addition, while LSTM models have been widely used, limited attention has been given to comparing their performance with other recurrent neural network architectures such as the GRU, which may offer advantages in computational efficiency and architectural simplicity. Therefore, this study aims to conduct a comprehensive comparison between LSTM and GRU models in predicting soil moisture using both univariate and multivariate approaches (integrated with climatic factors) across various prediction horizons.

2. RESEARCH METHODS

The research process includes collecting data from various trusted sources, pre-processing the data to improve dataset quality, dividing the data into training and test sets, and modeling and evaluating the model's performance.

2.1 Dataset

The data used in this study cover the East Java Province, Indonesia, using soil moisture data and climate variables. The data and data sources used in this study are as follows. The data and data sources used in this study are as follows:

1. Soil moisture data from July 1, 2019, to June 30, 2024, was obtained through Google Earth Engine (GEE), which integrates various satellite data sources, including SMAP, with a spatial resolution of 10 km × 10 km and a temporal resolution of 2-3 days.
2. Climate data including rainfall (mm), average humidity (%), minimum temperature (°C), maximum temperature (°C), average temperature (°C), duration of sunshine (hours), maximum wind speed (m/s), and average wind speed (m/s), were obtained from 10 meteorological stations in

East Java Province through the official website of the Meteorology, Climatology, and Geophysics Agency (BMKG) at https://dataonline.bmkg.go.id for the same observation period, from July 1, 2019 to June 30, 2024.

2.2 Research Stage

This research was conducted through several stages: data collection, data preprocessing, data split into training and test sets, modeling using LSTM and GRU algorithms, both with and without climate features, and model testing and evaluation to assess prediction performance. The research stages are shown in Fig. 1.

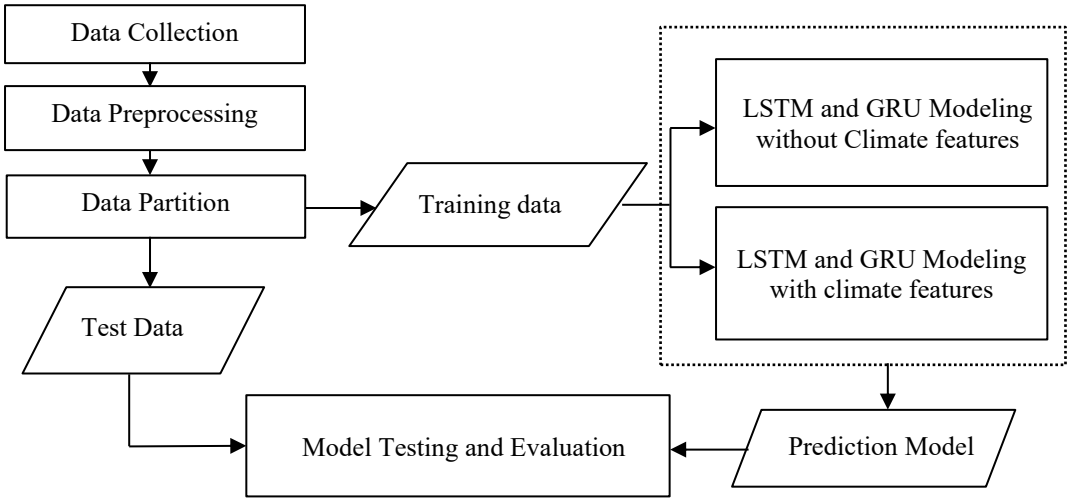

Figure 1. Research Stage

2.2.1 Data Collection

Soil moisture data were obtained from Google Earth Engine (SMAP) in 10 km × 10 km resolution for the period July 1, 2019 - June 30, 2024. Climate data (rainfall, temperature, humidity, solar irradiation, wind speed) were downloaded from BMKG for 10 stations in East Java during the same period.

2.2.2 Data Preprocessing

Pre-processing includes descriptive analysis, outlier detection with boxplots, and handling missing values using cubic spline interpolation. This method performs well at handling missing values [19]. Cubic spline interpolation technique can be calculated using Eq. (1) [20].

$$s_i(x) = a_i(x - x_i)^3 + b_i(x - x_i)^2 + c_i(x - x_i) + d_i. \quad (1)$$

Next, the data are normalized using the min-max technique. Normalization is important to prevent variable bias in predictions [21]. Min-max normalization converts data to the 0-1 range according to Eq. (2) [22].

$$x' = \frac{x - x(\min)}{x(\max) - x(\min)}, \quad (2)$$

where:

x' : normalized value;

x : original value of the data;

$x(max)$: maximum value of the data set.

2.2.3 Data Partition

fter preprocessing, the data was split into two: 80% for training and 20% for testing. This proportion was chosen because it has been empirically proven to optimize model performance [23], [24].

2.2.4 Modeling Using with LSTM & GRU

Modeling is performed using the LSTM and GRU algorithms with the Keras library in Python. The purpose of modeling is to get the best model in predicting soil moisture at 10 stations in East Java Province. The model was built in two scenarios: univariate (soil moisture only) and multivariate (using climate variables). Hyperparameter tuning is done by grid search to determine the best parameter combination. The parameters used in the grid search are shown in Table 1 [25].

Table 1. Parameters of LSTM and GRU

LSTM parameters	GRU parameters	Description
LSTM neurons	GRU neurons	Number of neurons in LSTM/GRU layer
activation	activation	Activation function used
optimizer	optimizer	Optimizer used
dropout_rate	dropout_rate	Dropout ratio to avoid overfitting

LSTM was first proposed by Hochreiter and Schmidhuber (1997) as an extension of RNN to overcome vanishing gradients by adding memory cells. The LSTM architecture is well-suited for predicting time-series data due to its ability to retain long-term information [26]. The architecture of an LSTM is shown in Fig. 2.

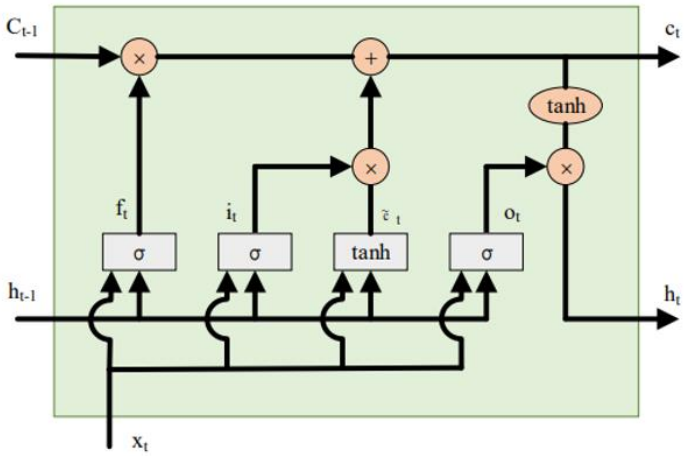

Figure 2. LSTM Architecture (Modified from [27])

Based on Fig. 2, the LSTM has three main gates: the forget gate, input gate, and output gate, which regulate the flow of information. Each gate is governed by sigmoid and tanh functions to control the information retained or forgotten at each iteration [13]. The equation of each gate can be seen in Eqs. (3)–(8).

1. forget gate $(f_t) = \sigma\left(W_f \cdot [h_{t-1}, x_t] + b_f\right)$, (3)
2. input gate $(i_t) = \sigma(W_i \cdot [h_{t-1}, x_t] + b_i)$, (4)

   output from input gate $(\tilde{C}_t) = tanh(W_C \cdot [h_{t-1}, x_t] + b_C)$, (5)

   cell state gate $(C_t) = \left(f_t \cdot C_{t-1} + i_t \cdot \tilde{C}_t\right)$, (6)
3. output gate $(o_t) = \sigma(W_o \cdot [h_{t-1}, x_t] + b_o)$, (7)
4. hidden state $(h_t) = o_t \cdot tanh(C_t)$, (8)

where:

σ : sigmoid activation function;

W_o, W_C, W_f, W_i: weight matrix of each gate;

h_{t-1} : hidden state at previous timestep;

x_t : input at current timestep;

b_o, b_C, b_f, b_i : bias of each gate.

Meanwhile, GRU was developed by [14] as a simpler version of LSTM. GRU has only an update gate and a reset gate, which combine the forget and input gate functions into a single mechanism. This structure makes GRU more computationally efficient, resulting in faster training time without sacrificing accuracy [15]. The architecture of the GRU is shown in Fig. 3.

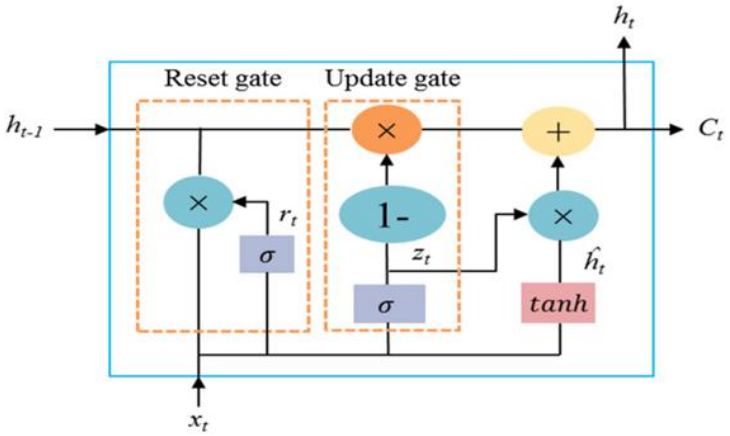

Figure 3. GRU Architecture (Modified from [28])

Fig. 3 shows the architecture of GRU, which processes input and hidden state through the reset gate and the update gate. The calculation process in GRU involves pointwise addition ($\oplus$) and pointwise multiplication ($\odot$) operations to combine old and new information into the current state [14]. The equations for each gate are given in Eqs. (9) – (12).

1. reset gate $(\mathrm{r_t}) = \sigma(\mathrm{W_r} \cdot [\mathrm{h_{t-1}}, \mathrm{x_t}] + \mathrm{b_r})$, (9)
2. update gate $(\mathrm{z_t}) = \sigma\left(\mathrm{W_z} \cdot [\mathrm{h_{t-1}}, \mathrm{x_t}] + \mathrm{b_z}\right)$, (10)

new memory $(\tilde{\mathrm{h}}_\mathrm{t}) = \tanh(\mathrm{W} \cdot [\mathrm{r_t} \odot \mathrm{h_{t-1}}, \mathrm{x_t}] + \mathrm{b})$, (11)

current state $(h_t) = z_t \odot h_{t-1} + (1 - z_t) \odot \tilde{h}_t$, (12)

where:

σ : sigmoid activation function (produces output between 0 and 1);

W_r, W_z, W : weights for reset gate;

h_{t-1} : hidden state at previous timestep;

x_t : input at timestep t;

b_r, b_z, b : bias of each gate.

2.2.5 Model Evaluation

Model evaluation is performed using several metrics, namely R-square (R^2), MAE, MAPE, MSE, and RMSE. R^2 is used to measure how well the model explains the variability in the data, with values close to 1 indicating better predictive performance [29]. MAE calculates the average absolute error between predicted and actual values, whereas MAPE measures the error as a percentage for easier interpretation [30]. MSE calculates the average squared error, and RMSE is the square root of MSE, scaling back to the original units of the data. These metrics are used to assess the predictive performance of the LSTM and GRU models in this study, calculated using Eqs. (13) – (17).

$$R^2 = \frac{\sum_{i=1}^{n}(y_i - \bar{y})^2 - \sum_{i=1}^{n}(y_i - \hat{y}_i)^2}{\sum_{i=1}^{n}(y_i - \bar{y})^2}, \quad (13)$$

$$MAE = \frac{1}{n}\sum_{i=1}^{n}|y_i - \hat{y}_i|, \quad (14)$$

$$MAPE = \frac{1}{n}\sum_{i=1}^{n}\left|\frac{y_i - \hat{y}_i}{y_i}\right| \times 100\%, \quad (15)$$

$$MSE = \frac{1}{n}\sum_{i=1}^{n}(y_i - \hat{y}_i)^2, \quad (16)$$

$$RMSE = \sqrt{\frac{1}{n}\sum_{i=1}^{n}(y_i - \hat{y}_i)^2}. \quad (17)$$

where:

y_i : the observed value for the *i*th observation;

$\hat{y}_i$: the predicted value for the *i*th observation;

$\bar{y}$: the average of all observed values;

n : the total number of data points.

3. RESULTS AND DISCUSSION

3.1 Data Collection

Data collection was carried out by downloading climate data from 10 BMKG stations located in East Java Province, namely: Malang Geophysics Station, Nganjuk Geophysics Station, Pasuruan Geophysics Station, East Java Climatology Station, Banyuwangi Meteorology Station, Juanda Meteorology Station, Tanjung Perak Maritime Meteorology Station, Perak I Meteorology Station, Trunojoyo Meteorology Station, and Tuban Meteorology Station. Soil moisture data were obtained from the Google Earth Engine (GEE) platform and matched to the coordinates of each BMKG station. All datasets were then merged using Microsoft Excel, separately for each station. The combined dataset for each station consists of 1828 rows × 9 columns, representing daily records from July 1, 2019, to June 30, 2024. The data were processed separately for each station because both LSTM and GRU models are time-series-based and highly dependent on the temporal patterns and continuity of data at each specific location.

3.2 Data Preprocessing

The data preprocessing stage begins with identifying and handling missing values to ensure data completeness. The number of missing values varied across variables, including the rainfall variable. Missing value handling was performed using the Cubic Spline Interpolation method. This method constructs a smooth, continuous interpolation function using cubic polynomials to estimate missing values. Cubic Spline Interpolation works by dividing the data range into intervals between known data points and fitting a third-degree (cubic) polynomial to each interval. The method ensures that the resulting curve is smooth at the boundaries, meaning the first and second derivatives are continuous across all intervals. This results in more natural and accurate estimates than linear interpolation, especially when the data exhibit non-linear patterns. The selection of the Cubic Spline Interpolation method is based on the study by [19], which showed that Spline Interpolation outperformed IL and ISt in handling missing values.

As shown in Fig. 4, the missing rainfall data for several dates from 2019 to 2024 were imputed using the cubic spline interpolation method. The green dots in the graph indicate the previously missing values that have been filled, while the blue line represents the actual rainfall data. The results show that the green dots blend smoothly with the blue line's pattern, thereby preserving the trend and continuity of the time series. This approach provides a more realistic approach to filling missing data than relying solely on simple averages or constant values.

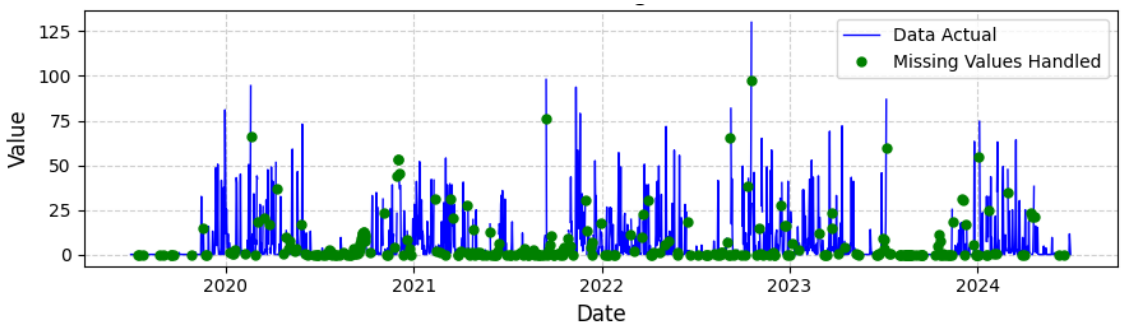

Figure 4. Visualization of Rainfall Data and Handled Missing Values Using Cubic Spline Interpolation

After handling missing values, the data is normalized using Min-Max scaling so that each feature is in the range [0, 1]. Normalization is important to speed up model training and avoid the dominance of certain features caused by scale differences. This process is applied consistently to training and testing data to maintain model integrity.

3.3 Data Partition

The dataset is split into two parts: 80% for training and 20% for testing. This division aims to ensure that the model has sufficient data to learn underlying patterns and dependencies during the training phase [23]. At the same time, the reserved test set enables an objective evaluation of the model's generalization capability on unseen data. By separating the training and test sets, it is possible to assess whether the model performs well not only on the data it was trained on but also on new, real-world data, thereby avoiding overfitting and ensuring more reliable predictive performance.

3.4 Modeling with LSTM and GRU

Soil moisture prediction modeling is performed using LSTM and GRU algorithms implemented with the TensorFlow-based Keras library in Python. The model is designed to predict soil moisture for the 1-10 days horizon at 10 BMKG stations in East Java using univariate and multivariate approaches. The LSTM and GRU model architectures for the two scenarios can be seen in Table 2 and Table 3. Each station was modeled and tested separately to capture local characteristics. Prediction is performed using a direct strategy, focusing on specific forecast horizons and minimizing accumulated error.

Based on Table 2 and Table 3, architecture of the LSTM and GRU models used in this study to predict soil moisture values using two approaches: univariate and multivariate. In the univariate approach, the model only receives 1 input feature in the form of daily soil moisture data, so the input layer consists of one node. In addition, in the multivariate approach, the model receives nine input features, consisting of one soil moisture variable and eight climate variables, namely minimum temperature (Tn), maximum temperature (Tx), average temperature (Tavg), average humidity (RH_avg), rainfall (RR), length of sunshine (ss), maximum wind speed (ff_x), and average wind speed (ff_avg). With this architecture, it is necessary to tune the model parameters to achieve optimal prediction performance. Hyperparameter tuning is performed using grid search to find the optimal parameter combination. The parameters used in the grid search are shown in Table 4.

Table 2. Univariate and Multivariate LSTM Architecture

Characteristic	Multivariate Specification	Univariate Specification
Architecture	1 input layer, 9 nodes 1 LSTM layer 1 dropout layer 1 dense layer 1 output layer	1 input layer, 1 node 1 LSTM layer 1 dropout layer 1 dense layer 1 output layer
Activation Function	relu, tanh	relu, tanh
Optimizer	adam, rmsprop	adam, rmsprop

Table 3. Univariate and Multivariate GRU Architecture

Characteristic	Multivariate Specification	Univariate Specification
Architecture	1 input layer, 9 nodes 1 GRU layer 1 dropout layer 1 dense layer 1 output layer	1 input layer, 1 node 1 GRU layer 1 dropout layer 1 dense layer 1 output layer
Activation Function	relu, tanh	relu, tanh
Optimizer	adam, rmsprop	adam, rmsprop

Table 4. List of Parameter Values for Grid Search in LSTM and GRU Modeling

Parameter	Values
Number of neurons	50, 100, 150
Activation	relu, tanh
Optimizer	adam, rmsprop
Dropout_rate	0.01; 0.2; 0.5

Based on Table 4, the parameters used in the hyperparameter tuning process for LSTM and GRU models include the number of neurons (50, 100, 150) to determine the number of neurons in the hidden layer, activation (relu, tanh) that play a role in determining the non-linearity of the learning process, optimizer (adam, rmsprop) used to optimize weight updates during training, and dropout_rate (0.01; 0.2; 0.5) applied to reduce the risk of overfitting by randomly ignoring some neurons during training. The LSTM and GRU architectures were designed with 50 epochs and 32 batch_sizes. Parameter adjustment is performed using the grid search method, which evaluates all possible parameter combinations to find the best configuration. The main objective is to find a set of parameters that yields the best predictive performance from the LSTM and GRU models using the available training data.

After the grid search identifies the best parameter combination, the model is trained on 80% of the dataset (training data), with the remaining 20% used for testing. This training process aims to enable the model to learn sequential patterns from historical soil moisture data and climate factors, while reserving unseen data for evaluating its generalization. After the model has been trained, it is tested on test data that was not used during training to evaluate its generalization to new data. The modeling results are presented in four tables, each showing the RMSE and $\boldsymbol{R^2}$ values for the univariate LSTM (Table 5), multivariate LSTM (Table 6), univariate GRU (Table 7), and multivariate GRU (Table 8) models for each station and prediction horizon.

Table 5. RMSE and R^2 Values for Univariate LSTM Soil Moisture Prediction at All Stations for Prediction Horizons of 1, 4, 7, and 10 Days

Station	Metric	Day			
		1	4	7	10
Malang Geophysical	RMSE	0.038	0.074	0.091	0.104
	R^2	0.956	0.828	0.741	0.667
Nganjuk Geophysical	RMSE	0.035	0.066	0.08	0.092
	R^2	0.985	0.945	0.919	0.893
Pasuruan Geophysical	RMSE	0.037	0.057	0.068	0.085
	R^2	0.984	0.963	0.948	0.918
Jawa Timur Climatological	RMSE	0.043	0.08	0.092	0.103
	R^2	0.976	0.918	0.89	0.864
Banyuwangi Meteorological	RMSE	0.052	0.091	0.101	0.108
	R^2	0.827	0.464	0.344	0.25
Juanda Meteorological	RMSE	0.028	0.054	0.068	0.082
	R^2	0.99	0.962	0.941	0.915
Maritim Tanjung Perak Meteorological	RMSE	0.041	0.086	0.098	0.103
	R^2	0.981	0.919	0.895	0.883

Station	Metric	Day			
		1	4	7	10
Perak I Meteorological	RMSE	0.041	0.085	0.097	0.105
	R^2	0.981	0.92	0.897	0.878
Trunojoyo Meteorological	RMSE	0.046	0.08	0.091	0.098
	R^2	0.953	0.859	0.818	0.789
Tuban Meteorological	RMSE	0.042	0.075	0.088	0.098
	R^2	0.974	0.918	0.887	0.86

Table 6. MSE and R^2 Values for Multivariate LSTM Soil Moisture Prediction at All Stations for Prediction Horizons of 1, 4, 7, and 10 Days

Station	Metric	Day			
		1	4	7	10
Malang Geophysical	RMSE	0.038	0.071	0.089	0.098
	R^2	0.955	0.843	0.756	0.7
Nganjuk Geophysical	RMSE	0.034	0.064	0.076	0.086
	R^2	0.985	0.947	0.926	0.906
Pasuruan Geophysical	RMSE	0.037	0.062	0.082	0.11
	R^2	0.985	0.956	0.925	0.862
Jawa Timur Climatological	RMSE	0.042	0.076	0.087	0.094
	R^2	0.978	0.925	0.903	0.886
Banyuwangi Meteorological	RMSE	0.054	0.09	0.104	0.105
	R^2	0.814	0.48	0.304	0.288
Juanda Meteorological	RMSE	0.028	0.053	0.063	0.07
	R^2	0.99	0.964	0.95	0.937
Maritim Tanjung Perak Meteorological	RMSE	0.04	0.084	0.094	0.096
	R^2	0.983	0.923	0.903	0.899
Perak I Meteorological	RMSE	0.041	0.084	0.096	0.1
	R^2	0.982	0.923	0.898	0.89
Trunojoyo Meteorological	RMSE	0.047	0.076	0.087	0.09
	R^2	0.951	0.871	0.831	0.82
Tuban Meteorological	RMSE	0.041	0.073	0.087	0.091
	R^2	0.975	0.921	0.89	0.878

Table 7. RMSE and R^2 Values for Univariate GRU Soil Moisture Prediction at All Stations for Prediction Horizons of 1, 4, 7, and 10 Days

Station	Metric	Day			
		1	4	7	10
Malang Geophysical	RMSE	0.036	0.073	0.092	0.105
	R^2	0.959	0.833	0.735	0.661
Nganjuk Geophysical	RMSE	0.033	0.065	0.079	0.09
	R^2	0.986	0.947	0.921	0.896
Pasuruan Geophysical	RMSE	0.036	0.056	0.069	0.084
	R^2	0.985	0.964	0.946	0.921
Jawa Timur Climatological	RMSE	0.042	0.08	0.092	0.104
	R^2	0.977	0.917	0.89	0.861
Banyuwangi Meteorological	RMSE	0.052	0.091	0.101	0.108
	R^2	0.827	0.466	0.336	0.249

Station	Metric	Day			
		1	4	7	10
Juanda Meteorological	RMSE	0.026	0.054	0.067	0.081
	R^2	0.991	0.963	0.944	0.917
Maritim Tanjung Perak Meteorological	RMSE	0.04	0.084	0.097	0.105
	R^2	0.983	0.923	0.897	0.878
Perak I Meteorological	RMSE	0.04	0.085	0.098	0.105
	R^2	0.983	0.921	0.895	0.88
Trunojoyo Meteorological	RMSE	0.046	0.079	0.091	0.099
	R^2	0.954	0.862	0.818	0.784
Tuban Meteorological	RMSE	0.042	0.074	0.088	0.098
	R^2	0.974	0.919	0.887	0.859

Table 8. RMSE and R^2 Values for Multivariate GRU Soil Moisture Prediction at All Stations for Prediction Horizons of 1. 4. 7. and 10 Days

Station	Metric	Day			
		1	4	7	10
Malang Geophysical	RMSE	0.036	0.072	0.088	0.1
	R^2	0.96	0.84	0.762	0.69
Nganjuk Geophysical	RMSE	0.034	0.064	0.077	0.086
	R^2	0.986	0.948	0.925	0.906
Pasuruan Geophysical	RMSE	0.036	0.062	0.086	0.109
	R^2	0.985	0.956	0.917	0.865
Jawa Timur Climatological	RMSE	0.042	0.076	0.088	0.092
	R^2	0.978	0.925	0.9	0.891
Banyuwangi Meteorological	RMSE	0.051	0.089	0.101	0.104
	R^2	0.832	0.49	0.339	0.304
Juanda Meteorological	RMSE	0.025	0.053	0.062	0.07
	R^2	0.992	0.965	0.952	0.937
Maritim Tanjung Perak Meteorological	RMSE	0.039	0.083	0.094	0.097
	R^2	0.983	0.925	0.904	0.897
Perak I Meteorological	RMSE	0.04	0.083	0.096	0.1
	R^2	0.982	0.925	0.9	0.89
Trunojoyo Meteorological	RMSE	0.046	0.077	0.087	0.091
	R^2	0.954	0.87	0.833	0.819
Tuban Meteorological	RMSE	0.042	0.074	0.087	0.092
	R^2	0.974	0.92	0.89	0.876

Based on Table 5, Table 6, Table 7, and Table 8, all models (univariate LSTM, multivariate LSTM, univariate GRU, and multivariate GRU) demonstrate good soil moisture prediction performance at most stations. particularly for short-term horizons (t+1) with R^2 values above 0.90 and low RMSE. However. accuracy tends to decrease as the prediction horizon increases. Among the four models, the multivariate GRU shows the best overall performance, with high R^2 values and low RMSE at many stations, especially for short- to medium-term horizons. The univariate and multivariate LSTM models also produce competitive results. Although their performance at some stations is slightly below that of the multivariate GRU. The univariate GRU tends to produce smoother predictions, but its R^2 decreases more sharply over longer horizons. Stations such as Juanda Meteorological Station are examples of locations with very high performance across all models. while Banyuwangi Meteorological Station consistently shows the lowest accuracy.

3.5 Model Evaluation

evaluated using several metrics. namely MAE, MSE, RMSE, MAPE, and R^2. The 5 metrics are calculated from the average of the predicted results across 10 observation stations and 10 times horizons (t to t+9). The performance comparison for each metric is presented sequentially: Fig. 5 illustrates the average MAE values. Fig.6 displays the MSE. Fig. 7 shows the RMSE. Fig. 8 presents the MAPE. and Fig. 9 depicts the R^2 values. Fig. 10 illustrates the training time (in seconds) of each model at each station, highlighting computational efficiency differences across models and locations.

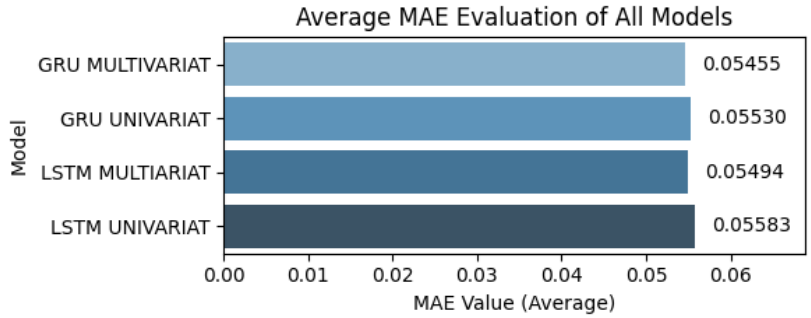

Figure 5. Comparison of Average MAE Values of LSTM and GRU Models

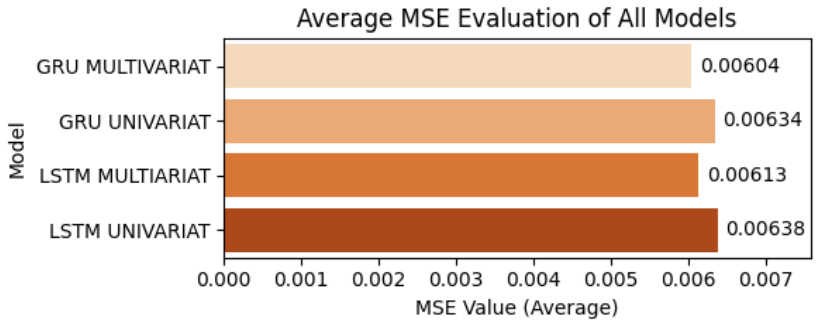

Figure 6. Comparison of Average MSE Values of LSTM and GRU Models

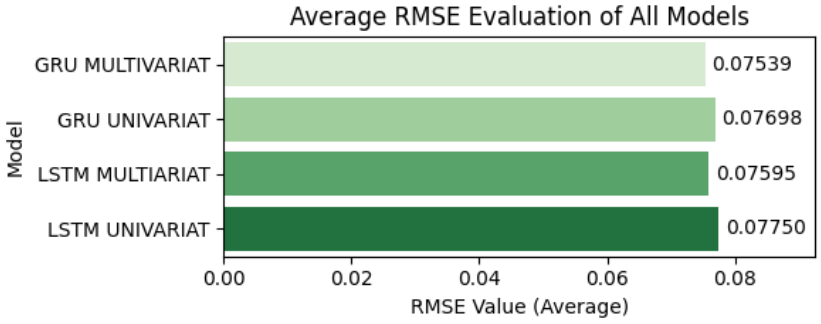

Figure 7. Comparison of Average Values of RMSE of LSTM and GRU Models

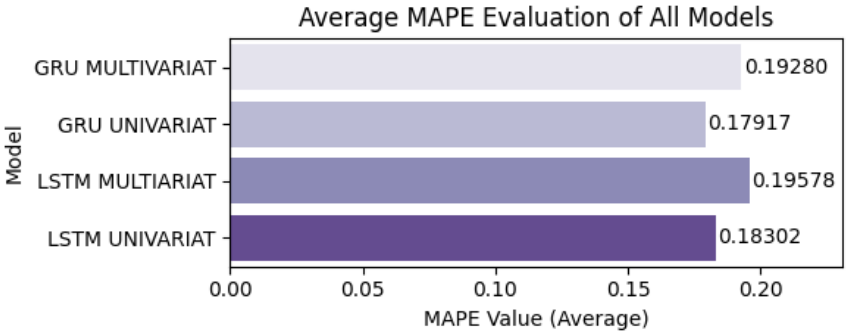

Figure 8. Comparison of the Average Value of MAPE LSTM and GRU Models

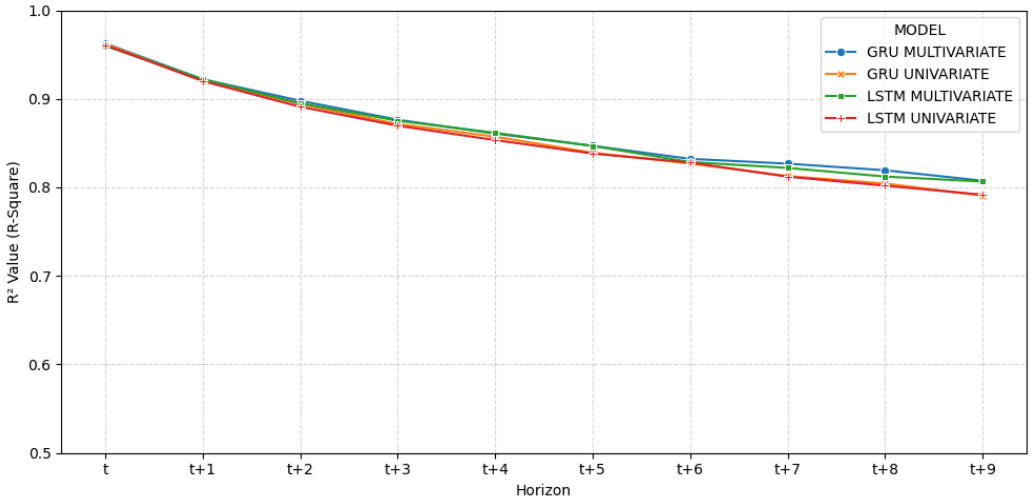

Figure 9. Comparison of the Average Value of R² LSTM and GRU Models

Based on the average evaluation results of the five-performance metrics (MAE, MSE, RMSE, R^2, and MAPE) shown in Fig. 5, Fig. 6, Fig. 7, Fig. 8, and Fig. 9, the multivariate GRU model consistently shows the most superior performance compared to other models. In the MAE metric, multivariate GRU obtained the lowest value of 0.05455, followed by multivariate LSTM (0.05494), univariate GRU (0.05530), and univariate LSTM (0.05583). Similar results were also seen in the MSE metric, where multivariate GRU again recorded the lowest value of 0.00604, slightly better than multivariate LSTM (0.00613), univariate GRU (0.00634), and univariate LSTM (0.00638). On the RMSE metric, multivariate GRU recorded an average of 0.07539, indicating a consistently low error rate, followed by multivariate LSTM (0.07595), and univariate GRU (0.07698), while univariate LSTM obtained the highest value of 0.07750. In terms of relative accuracy based on percentage error (MAPE), multivariate GRU is again the best model with a value of 0.19280, followed by multivariate LSTM (0.19578), univariate LSTM (0.18302), and univariate GRU (0.17917).

The consistency of the multivariate GRU's performance is also evident in the R² metric shown in Fig. 10. The model recorded an R² of 0.9626 at the day 1 horizon and maintained an R² of 0.8075 at day 10. This shows that the multivariate GRU not only achieves the lowest prediction error but also demonstrates better long-term prediction stability.

Overall, the multivariate GRU is recommended as the most reliable model for daily soil moisture prediction based on meteorological data, especially in the multivariate scenario with a prediction horizon of up to 10 days ahead. The model shows a balance between prediction accuracy, performance stability, and generalization efficiency. However, for short-term prediction needs, univariate GRU can also be an alternative with competitive performance.

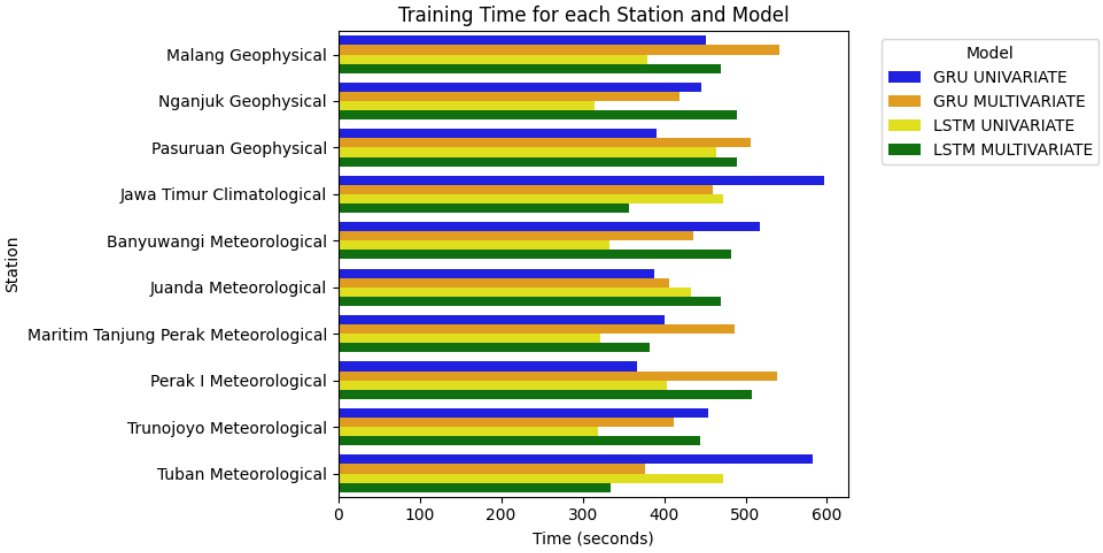

Figure 10. Training Time for Each Station and Model

Based on Fig. 10, the multivariate GRU has the longest training time. reaching more than 550 seconds at stations such as Geofisika Malang and Meteorology Tuban. This is due to the model's complexity, which processes many features at once. Multivariate LSTM models are more efficient than multivariate GRU, with training times generally under 500 seconds. Meanwhile, the univariate LSTM and univariate GRU showed the fastest training times. The univariate GRU even recorded times below 300 seconds at some stations.

Overall, the multivariate model is more accurate but requires longer training time, while the univariate model is more computationally efficient. Therefore, model selection should balance accuracy and efficiency.

4. CONCLUSION

This study has successfully built a daily soil moisture prediction model based on deep learning algorithms LSTM and GRU, both in univariate and multivariate scenarios, by integrating climate variables from 10 meteorological stations in East Java Province. Evaluation results using five metrics (MAE, MSE, RMSE, MAPE, and R^2) indicated that the multivariate GRU model was the best-performing. This model yielded the lowest error values (MAE = 0.05455; MSE = 0.00604; RMSE = 0.07539; MAPE = 0.19280) and the highest long-term prediction stability (R^2 from 0.955 at t to 0.802 at t+9). The univariate GRU model also demonstrated strong performance at short prediction horizons. However, the fastest training time was recorded by the univariate LSTM model (<400 seconds). making it the most computationally efficient option. In contrast. multivariate models. especially the multivariate GRU. require longer training times (>550 seconds at some stations) due to the increased input complexity. Therefore, model selection should consider both the prediction time horizon and computational constraints. For medium to long-term forecasting, the multivariate GRU is recommended for its accuracy and stability. Meanwhile, for fast, efficient daily predictions, the univariate LSTM is a practical alternative. Future research should explore applications across different regions and climate conditions. with a focus on developing a real-time early warning system based on soil moisture prediction. In addition. Future studies are encouraged to expand the geographical coverage of datasets and investigate hybrid modeling approaches that combine the strengths of multiple algorithms to further enhance prediction accuracy and robustness. Researchers should also consider incorporating additional environmental variables and testing transfer learning techniques for regions with limited data. and evaluating model performance under extreme climate events to ensure broader applicability and resilience.

Author Contributions

Jemsri Stenli Batlajery: Conceptualization, Data Curation, Software, Methodology, Visualization, Formal Analysis, Writing – Original Draft. Agus Buono: Supervision, Project Administration, Validation, Resources, Writing –Review and Editing. Mushthofa: Supervision, Validation, Resources, Writing – Review and Editing. All authors discussed the results, contributed to the interpretation of the data, and approved the final version of the manuscript.

Funding Statement

This research received no specific grant from any public funding agency, commercial, or not-for-profit sectors.

Acknowledgment

The research team would like to express our deepest gratitude to the individuals and institutions that have made important contributions to the success of our research.

Declarations

The authors declare no competing interests.

Declaration of Generative AI and AI-assisted technologies

The authors declare that no generative AI or AI-assisted technologies were used in the preparation of this manuscript, including for writing, editing, data analysis, or the creation of tables and figures.

REFERENCES

[1] KEMENTAN Keputusan Menteri Pertanian, *RENCANA STRATEGIS KEMENTRIAN PERTANIAN TAHUN 2020-2024*. Jakarta: Kementan, 2021.

[2] N. Pareek, "CLIMATE CHANGE IMPACT ON SOILS: ADAPTATION AND MITIGATION," *MOJ Ecol. Environ. Sci.*, vol. 2, no. 3, pp. 136–139, 2017, doi: https://doi.org/10.15406/mojes.2017.02.00026.

[3] M. T. Taye, E. Dyer, F. A. Hirpa, and K. Charles, "CLIMATE CHANGE IMPACT ON WATER RESOURCES IN THE AWASH BASIN, ETHIOPIA," *Water (Switzerland)*, vol. 10, no. 11, pp. 1–16, 2018, doi: https://doi.org/10.3390/w10111560.

[4] S. M. Mostafa, O. Wahed, W. Y. El-Nashar, S. M. El-Marsafawy, M. Zelenáková, and H. F. Abd-Elhamid, "ERRATUM TO: POTENTIAL CLIMATE CHANGE IMPACTS ON WATER RESOURCES IN EGYPT (WATER 2021, 13, 1715)," *Water (Switzerland)*, vol. 13, no. 14, 2021, doi: https://doi.org/10.3390/w13141919.

[5] G. S. Malhi, M. Kaur, and P. Kaushik, "IMPACT OF CLIMATE CHANGE ON AGRICULTURE AND ITS MITIGATION STRATEGIES: A REVIEW," *Sustain.*, vol. 13, no. 3, pp. 1–21, 2021, doi: https://doi.org/10.3390/su13031318.

[6] S. Fawzy, A. I. Osman, J. Doran, and D. W. Rooney, "STRATEGIES FOR MITIGATION OF CLIMATE CHANGE: A REVIEW," *Environ. Chem. Lett.*, vol. 18, no. 6, pp. 2069–2094, 2020, doi: https://doi.org/10.1007/s10311-020-01059-w.

[7] L. Myeni, M. E. Moeletsi, and A. D. Clulow, "PRESENT STATUS OF SOIL MOISTURE ESTIMATION OVER THE AFRICAN CONTINENT," *J. Hydrol. Reg. Stud.*, vol. 21, no. December 2018, pp. 14–24, 2019, doi: https://doi.org/10.1016/j.ejrh.2018.11.004.

[8] S. J. Sutanto *et al.*, "THE ROLE OF SOIL MOISTURE INFORMATION IN DEVELOPING ROBUST CLIMATE SERVICES FOR SMALLHOLDER FARMERS: EVIDENCE FROM GHANA," *Agronomy*, vol. 12, no. 2, 2022, doi: https://doi.org/10.3390/agronomy12020541.

[9] L. Zhang *et al.*, "IN SITU OBSERVATION-CONSTRAINED GLOBAL SURFACE SOIL MOISTURE USING RANDOM FOREST MODEL," *Remote Sens.*, vol. 13, no. 23, pp. 1–25, 2021, doi: https://doi.org/10.3390/rs13234893.

[10] L. Gałęzewski *et al.*, "ANALYSIS OF THE NEED FOR SOIL MOISTURE, SALINITY AND TEMPERATURE SENSING IN AGRICULTURE: A CASE STUDY IN POLAND," *Sci. Rep.*, vol. 11, no. 1, 2021, doi: https://doi.org/10.1038/s41598-021-96182-1.

[11] N. Sazib, J. D. Bolten, and I. E. Mladenova, "LEVERAGING NASA SOIL MOISTURE ACTIVE PASSIVE FOR ASSESSING FIRE SUSCEPTIBILITY AND POTENTIAL IMPACTS OVER AUSTRALIA AND CALIFORNIA," *IEEE J. Sel. Top. Appl. Earth Obs. Remote Sens.*, vol. 15, no. June, pp. 779–787, 2022, doi: https://doi.org/10.1109/JSTARS.2021.3136756.

[12] S. H. Noh, "ANALYSIS OF GRADIENT VANISHING OF RNNS AND PERFORMANCE COMPARISON," *Inf.*, vol. 12, no. 11, 2021, doi: https://doi.org/10.3390/info12110442.

[13] S. Hochreiter and J. Schmidhuber, "LONG SHORT-TERM MEMORY," *Neural Comput.*, vol. 9, no. 8, pp. 1735–1780, 1997, doi: https://doi.org/10.1162/neco.1997.9.8.1735.

[14] J. Chung, C. Gulcehre, K. Cho, and Y. Bengio, "EMPIRICAL EVALUATION OF GATED RECURRENT NEURAL NETWORKS ON SEQUENCE MODELING," pp. 1–9, 2014, [Online]. Available: http://arxiv.org/abs/1412.3555

[15] K. E. ArunKumar, D. V. Kalaga, C. Mohan Sai Kumar, M. Kawaji, and T. M. Brenza, "COMPARATIVE ANALYSIS OF GATED RECURRENT UNITS (GRU), LONG SHORT-TERM MEMORY (LSTM) CELLS, AUTOREGRESSIVE INTEGRATED MOVING AVERAGE (ARIMA), SEASONAL AUTOREGRESSIVE INTEGRATED MOVING AVERAGE (SARIMA) FOR FORECASTING COVID-19 TRENDS," *Alexandria Eng. J.*, vol. 61, no. 10, pp. 7585–7603, 2022, doi: https://doi.org/10.1016/j.aej.2022.01.011.

[16] Y. Chen *et al.*, "CONVOLUTIONAL NEURAL NETWORK MODEL FOR SOIL MOISTURE PREDICTION AND ITS TRANSFERABILITY ANALYSIS BASED ON LABORATORY VIS-NIR SPECTRAL DATA," *Int. J. Appl. Earth Obs. Geoinf.*, vol. 104, no. September, p. 102550, 2021, doi: https://doi.org/10.1016/j.jag.2021.102550.

[17] N. Filipović, S. Brdar, G. Mimić, O. Marko, and V. Crnojević, "REGIONAL SOIL MOISTURE PREDICTION SYSTEM BASED ON LONG SHORT-TERM MEMORY NETWORK," *Biosyst. Eng.*, vol. 213, pp. 30–38, 2022, doi: https://doi.org/10.1016/j.biosystemseng.2021.11.019.

[18] M. F. Celik, M. S. Isik, O. Yuzugullu, N. Fajraoui, and E. Erten, "SOIL MOISTURE PREDICTION FROM REMOTE SENSING IMAGES COUPLED WITH CLIMATE, SOIL TEXTURE AND TOPOGRAPHY VIA DEEP LEARNING," *Remote Sens.*, vol. 14, no. 21, pp. 1–24, 2022, doi: https://doi.org/10.3390/rs14215584.

[19] M. Haikal, "PENGEMBANGAN MODEL PRAPROSES DATA DAN MODEL PREDIKSI TINGGI MUKA AIR TANAH GAMBUT DENGAN ALGORITMA LSTM [TESIS]," IPB University, 2023.

[20] S. McKinley and M. Levine, "CUBIC SPLINE INTERPOLATION," *Methods Shape-Preserving Spline Approx.*, vol. 3, no. 2, pp. 37–59, 1998, doi: https://doi.org/10.1142/9789812813381_0003.

[21] C. Biele, J. Kacprzyk, W. Kopeć, J. W. Owsiński, A. Romanowski, and M. Sikorski, *DIGITAL INTERACTION AND MACHINE INTELLIGENCE*, Volume 440. Warsaw, Poland: Springer, 2021. [Online]. Available: https://link.springer.com/bookseries/15179

[22] N. Mahesh, J. J. Babu, K. Nithya, and S. A. Arunmozhi, "WATER QUALITY PREDICTION USING LSTM WITH COMBINED NORMALIZER FOR EFFICIENT WATER MANAGEMENT," *Desalin. Water Treat.*, vol. 317, no. January, p. 100183, 2024, doi: https://doi.org/10.5772/intechopen.72352.

[23] B. Vrigazova, "THE PROPORTION FOR SPLITTING DATA INTO TRAINING AND TEST SET FOR THE BOOTSTRAP IN CLASSIFICATION PROBLEMS," *Bus. Syst. Res.*, vol. 12, no. 1, pp. 228–242, 2021, doi: https://doi.org/10.2478/bsrj-2021-0015.

[24] A. Gholamy, V. Kreinovich, and O. Kosheleva, "WHY 70/30 OR 80/20 RELATION BETWEEN TRAINING AND TESTING SETS : A PEDAGOGICAL EXPLANATION," *Dep. Tech. Reports*, vol. 1209, pp. 1–6, 2018.

[25] S. Kervanci and M. F. Akay, "LSTM HYPERPARAMETERS OPTIMIZATION WITH HPARAM PARAMETERS FOR BITCOIN PRICE PREDICTION," 2023, doi: https://doi.org/10.35377/saucis...1172027.

[26] Z. C. Lipton, J. Berkowitz, and C. Elkan, "A CRITICAL REVIEW OF RECURRENT NEURAL NETWORKS FOR SEQUENCE LEARNING," pp. 1–38, 2015, [Online]. Available: http://arxiv.org/abs/1506.00019

[27] J. Luo, L. Zhu, K. Zhang, C. Zhao, and Z. Liu, "FORECASTING THE 10.7-CM SOLAR RADIO FLUX USING DEEP CNN-LSTM NEURAL NETWORKS," *Processes*, vol. 10, no. 2, pp. 1–11, 2022, doi: https://doi.org/10.3390/pr10020262.

[28] S. Mohsen, "RECOGNITION OF HUMAN ACTIVITY USING GRU DEEP LEARNING ALGORITHM," *Multimed. Tools Appl.*, vol. 82, no. 30, pp. 47733–47749, 2023, doi: https://doi.org/10.1007/s11042-023-15571-y.

[29] D. Chicco, M. J. Warrens, and G. Jurman, "THE COEFFICIENT OF DETERMINATION R-SQUARED IS MORE INFORMATIVE THAN SMAPE, MAE, MAPE, MSE AND RMSE IN REGRESSION ANALYSIS EVALUATION," *PeerJ Comput. Sci.*, vol. 7, pp. 1–24, 2021, doi: https://doi.org/10.7717/PEERJ-CS.623.

[30] I. A. Zulfauzi, N. Y. Dahlan, H. Sintuya, and W. Setthapun, "ANOMALY DETECTION USING K-MEANS AND LONG-SHORT TERM MEMORY FOR PREDICTIVE MAINTENANCE OF LARGE-SCALE SOLAR (LSS) PHOTOVOLTAIC PLANT," *Energy Reports*, vol. 9, no. S12, pp. 154–158, 2023, doi: https://doi.org/10.1016/j.egyr.2023.09.159.